ELECTRIC CURRENTS INDUCED BY NON-PERIODIC WINDS IN THE IONOSPHERE, (I)

by

Hiroshi Maeda*

Institute for Space Studies
Goddard Space Flight Center, NASA
New York, New York

and

Hiroo Murata

Geophysical Institute
Kyoto University
Kyoto, Japan

*National Academy of Sciences - National Research Council Senior Research Associate with the Goddard Institute for Space Studies; on leave from Kyoto University.

ABSTRACT

Electric currents induced by non-periodic winds in the ionosphere are calculated for the case of incoincidence of the Earth's rotational and magnetic axes, based on a realistic model of the upper atmosphere. Main results obtained are as follows: (1) Sq-like current systems changing with universal time are produced and the intensity of main vortices is about one tenth of that of the Sq field for a typical wind velocity of 10 m/sec. (2) Of the two components of non-periodic winds the meridional component is more effective in producing current systems. (3) The position of main current vortices is controlled by the distributions of ionospheric conductivity and of wind velocity and the degree of influence of these two is different for different profiles of winds. (4) The intensity of main vortices changes with longitude in such a manner that the maximum intensity occurs in the north and south American zone and the minimum in the Asia and Oceania zone, being in agreement with that of the Sq field. (5) No remarkable difference can be seen in the results obtained by using different coordinate systems.

1. INTRODUCTION

The atmospheric dynamo theory was studied by a number of authors (see for example, a brief summary by Maeda, 1966) for interpreting the solar and lunar daily geomagnetic variations at the early stage, and for discussing dynamical behavior of the upper atmosphere at the latter. In most of these studies only periodic components of ionospheric winds which induced the so-called dynamo electric field were considered, because it has long been believed that ionospheric winds are of only or mainly tidal origin.

In recent years, however, thermally driven ionospheric winds have warmly been discussed, and it has been pointed out by Gupta (1967), for example, that the contribution of gravitational tide to (solar daily) geomagnetic variations would be negligible as compared with that of solar radiation. If it is so, the winds may have non-periodic components as well as periodic ones. In fact the results of observation of ionospheric motions by radio and rockets strongly suggest the existence of non-periodic components in ionospheric motions. Thus, it may be expected that electric currents might be induced by such non-periodic winds and may result in geomagnetic variations observed on the ground.

This problem was considered by Kato (1957) for a zonal wind, and by Jones (1963) and DeWitt and Akasofu (1964) for a solenoidal wind, and it was concluded by these authors that no total currents could be induced by such a zonal or solenoidal wind. Their discussions were made on some simplifying assumptions, especially it was assumed that the electric currents flowed in a thin layer in which the wind velocity and the electric field did not change with height (a two-dimensional assumption) and that a rotational and magnetic axes of the Earth were coincident (a coincident-axes assumption). There still, therefore, remains the possibility that a current system can be produced by non-periodic winds, for the case in which one or two of the above assumptions are not satisfied to a certain approximation. In fact, the results of estimate by Maeda and Matsumoto (1962) and by van Sabben (1962) seemed to suggest this possibility.

Maeda and Matsumoto considered the case in which the coincident-axes assumption did not hold, and they obtained current systems depending on universal time as well as local time. van Sabben discussed the case in which the two-dimensional assumption was violated, and he showed that certain height-dependent zonal or meridional wind distributions would

cause Sq-like current systems. These findings seem to be important in discussing not only the daily geomagnetic variations but also the dynamics of the upper atmosphere. Their numerical results, however, seem to be far from any realistic one, because the models employed were over-simplified.

The purpose of this series of papers is to discuss the method of mathematical treatment of the problem in a general form and then present numerical results based on a realistic model of the upper atmosphere. Part I deals with only the case of incoincidnet axes. The effect of height-dependent wind structure will be considered in Part II where the axes-incoincidence is ignored, and the most general case in which the above two cases are combined will finally be discussed in Part III.

2. TWO-DIMENSIONAL DYNAMO EQUATIONS

In the two-dimensional case, we take a hypothetical spherical current sheet which has a height-integrated tensor conductivity $[K]$, then the (height-integrated) current density $\vec{J}$ is given by

$$\vec{J} = [K]\,\vec{E}_t \qquad (1)$$

where $\vec{E}_t$ is the (height-independent) total electric field.

If we consider a quasi-steady state, the effect of self-inductance may be ignored, so that the total electric field is given by the sum of the electrostatic field $\vec{E}_s$ derived from a potential S and the dynamo electric field $\vec{E}_d$ (= $\vec{V} \times \vec{B}$; $\vec{V}$ is the wind velocity and $\vec{B}$ is the geomagnetic field intensity). Since displacement currents can be neglected in the present case, the current must be divergent free; i.e.,

$$\text{div } \vec{J} = 0. \qquad (2)$$

Taking spherical coordinates (co-latitude θ, longitude λ) and local Cartesian coordinates (x for southward, y for eastward) at a point (θ, λ) on the current sheet, we have from (1) and (2)

$$\alpha \frac{\partial^2 S}{\partial \theta^2} + \beta \frac{\partial^2 S}{\partial \lambda^2} + \gamma \frac{\partial S}{\partial \theta} + \delta \frac{\partial S}{\partial \lambda} = \varepsilon \qquad (3)$$

where

$$\alpha = K_{xx} \sin\theta, \qquad \beta = K_{yy} / \sin\theta$$
$$\gamma = \partial\alpha/\partial\theta - \partial K_{xy}/\partial\lambda$$
$$\delta = \partial K_{xy}/\partial\theta + \partial K_{yy}/(\sin\theta\, \partial\lambda)$$
$$\varepsilon = \partial F_x/\partial\theta + \partial F_y/\partial\lambda$$
$$F_x = a \sin\theta\, (K_{xx} E_{dx} + K_{xy} E_{dy})$$
$$F_y = a\, (-K_{xy} E_{dx} + K_{yy} E_{dy})$$
$$a = \text{radius of current sheet}$$

and K_{xx}, K_{yy} and K_{xy} are components of tensor conductivity [K] (see for example, Chapman, 1956). Since $\alpha\beta > 0$ this is a partial differential equation of elliptic type.

The electric conductivities (K_{xx} etc.) are, in general, functions of θ, λ and t (local time), but the dynamo field $\vec{E}_d$ does not depend on local time because only non-periodic winds are considered here. Thus eq. (3) may be written

$$\frac{\partial^2 S}{\partial \theta^2} + A\frac{\partial^2 S}{\partial \lambda^2} + B\frac{\partial S}{\partial \theta} + C\frac{\partial S}{\partial \lambda} = D \qquad (4)$$

where

$$A = \beta/\alpha = A(\theta, \lambda, t)$$
$$B = \gamma/\alpha = B(\theta, \lambda, t)$$
$$C = \delta/\alpha = C(\theta, \lambda, t)$$
$$D = \varepsilon/\alpha = D(\theta, \lambda, t)$$

and therefore the solution would be the form

$$S = S(\theta, \lambda, t). \qquad (5)$$

Eq. (4) is the basic equation in our problem, to be solved under appropriate boundary conditions.

In actual cases the coefficients, A, B, C and D cannot be expressed in any analytical forms but are given by numerical values, and therefore the solution is obtained by a method of numerical integration. When we carry out calculations,

an important question may arise, i.e., which of the geographic and geomagnetic coordinates is appropriate for the practical treatment ? We cannot briefly answer this question, and this will be discussed in the next section.

3. COORDINATE SYSTEMS AND BOUNDARY CONDITIONS

The physical quantities involved in eq. (4) are the wind velocity $\vec{V}$, the geomagnetic field intensity $\vec{B}$, the electrical conductivity [K] as known, and the electrostatic potential S as unknown. Of these, the wind velocity would be dependent on the geographical (gg) coordinates, and the geomagnetic field intensity depends, of course, upon the geomagnetic (gm) coordinates. Thus, if we take the gg coordinates, $\vec{B}$ must be transformed; whereas if we take the gm coordinates, $\vec{V}$ must be transformed. However, what about the electrical conductivity ? The electrical conductivity contains several quantities; some of them (for instance, the electron density or collision frequency) might be dependent on the gg coordinates, but the gyrofrequency would be in conformity with the gm coordinates. Thus it seems to be very hard to determine any one coordinate system appropriate for the conductivity. We know, however, that near the equator the conductivity is strongly controlled by the geomagnetic

field as well known as the equatorial electrojet phenomenon, whereas in high latitudes the gg coordinates might be better for the expression of conductivity, because the geomagnetic field is nearly vertical there.

We meet the same difficulty as above for the determination of boundary conditions. If we want to solve the basic equation in its original form, we must employ one of the following two kinds of boundary conditions: One is called a Dirichlet problem in which the values of the unknown at the boundary are known and the other is called a Neuman problem in which the values of the normal derivative of the unknown at the boundary are known. Unfortunately, our present problem is not so simple. The unknown S is a potential, so that we can take an arbitrary value of S at any one point. The north pole is usualy taken as this point. However, a difficulty again occurs, because the values of all the coefficients (A, B, C and D) in the equation tend to infinity at the pole, so that we cannot set any boundary conditions at the pole. Instead, the polar condition might be replaced by the values at points close to the pole, and these values may be estimated by Taylor expansion of S around the pole. This boundary condition would be better satisfied for the gg coor-

dinates rather than the gm coordinates.

On the other hand, at the equator we may take the condition that

$$\partial S/\partial \theta = 0$$

which is based on the assumption that the geomagnetic field lines can be regarded as equipotentials, and therefore this condition is satisfied for the gm equator not for the gg equator. Thus, we again meet a difficulty for the choice of coordinates appropriate for boundary conditions. Since it is impossible to take any combined coordinate system, calculations are carried out for each of the gg and gm coordinates. We would say therefore that the results taking the gg coordinates are doubtful near the equator, whereas the results taking the gm coordinates are less significant in the polar region.

Finally, for the east-west boundaries we set the condition

$$S \text{ (at } \lambda = 0) = S \text{ (at } \lambda = 2\pi)$$

because of the periodicity expected for S.

4. COORDINATE TRANSFORMATION

As discussed above, if we employ any one coordinate sys-

tem, some quantities must be transformed; i.e., if we take the gg coordinates, the geomagnetic field intensity $\vec{B}$ must be transformed; whereas if we take the gm coordinates, the wind velocity $\vec{V}$ must be transformed. The method of transformation is discussed below.

4. 1. General.

A general method for the coordinate transformation of any physical quantities as a function of position on a sphere may be provided by using the spherical surface harmonics (see, Schmidt, 1935).

Let N and N' in Fig. 1 be the north poles of any two coordinate systems (u,t) and (u',t'), we have

$$P_n^{\mu}(\cos u')\cos\mu t' = \sum_{m=0}^{n} A_{m\mu} P_n^{m}(\cos u)\cos mt$$
$$P_n^{\mu}(\cos u')\sin\mu t' = \sum_{m=0}^{n} B_{m\mu} P_n^{m}(\cos u)\sin mt \qquad (6)$$

where P_n^m are the semi-normalized associated Legendre functions introduced by Schmidt (1935), and A_n^m and B_n^m are given by

$$A_{m\mu} = A_{\mu m} = (a_{nm}\, a_{n\mu})^{\frac{1}{2}}\,(A + B)/2$$
$$B_{m\mu} = B_{\mu m} = (a_{nm}\, a_{n\mu})^{\frac{1}{2}}\,(A - B)/2$$
$$A = (1 - c)^{m} s^{\mu-m} \frac{d^{\mu}}{dc^{\mu}}\left[(1 + c)^{m} \frac{d^{m}P_n(c)}{d\,c^{m}}\right]$$

$$B = (1 + c)^{m} s^{\mu-m} \frac{d^{\mu}}{dc^{\mu}} \left[(1 - c)^{m} \frac{d^{m}P_n(c)}{d\, c^{m}} \right]$$

$c = \cos e$

$s = \sin e$

$a_{nm} = \varepsilon_m (n - m)!/(n + m)!$

$\varepsilon_o = 1, \quad \varepsilon_1 = \varepsilon_2 = \ldots\ldots\ldots = 2$

and $P_n(c)$ = Legendre functions.

These formulae are the most general expression for the transformation of spherical coordinates, and they are very useful for the present problem.

4. 2. Case where the gg coordinates are taken.

If we take

$$u = \theta, \qquad u' = \text{Ⓗ}$$

$$t = \lambda - \lambda_o, \qquad t' = \pi - \Lambda$$

$$e = \theta_o,$$

where (θ, λ) are the gg coordinates of point P (see Fig. 1), $(\text{Ⓗ}, \Lambda)$ are its gm coordinates, and (θ_o, λ_o) are the gg coordinates of the geomagnetic pole N', then we have from (6)

$$P_n^{\mu}(\cos \text{Ⓗ}) \cos \mu(\pi - \Lambda) = \sum_{m=o}^{n} A_{m\mu} P_{\mu}^{m}(\cos \theta) \cos m(\lambda - \lambda_o)$$

$$P_n^{\mu}(\cos \text{Ⓗ}) \sin \mu(\pi - \Lambda) = \sum_{m=o}^{n} B_{m\mu} P_{\mu}^{m}(\cos \theta) \sin m(\lambda - \lambda_o) \qquad (7)$$

The geomagnetic field intensity can, in general, be trans-

formed into the gg coordinates by these formulae.

As an example, if we approximate the geomagnetic field by a dipole field of magnetic moment $\vec{M}$, we have

$$B_z = -(2M/a^3)\ P_1^{\,0}(\cos\Theta)$$

for the vertical intensity. Application of (7) to $P_1^{\,0}(\cos\Theta)$ gives

$$\begin{aligned} P_1^{\,0}(\cos\Theta) &= P_1^{\,0}(c)\ P_1^{\,0}(\cos\theta) \\ &\quad + P_1^{\,1}(c)\ P_1^{\,1}(\cos\theta)\ \cos(\lambda-\lambda_o) \\ &= \cos\theta_o\cos\theta + \sin\theta_o \sin\theta \cos(\lambda-\lambda_o) \end{aligned}$$

it follows that

$$B_z = -(2M/a^3)\left[\cos\theta_o\cos\theta + \sin\theta_o \sin\theta \cos(\lambda-\lambda_o)\right].$$

This is the well known expression for the vertical intensity of the goemagnetic field transformed into the gg coordinates.

4. 3. Case where the qm coordinates are taken.

The inverse transformation to the above can be obtained by changing

$$t \rightleftarrows t', \quad u \rightleftarrows u'$$

and again by taking

$$\begin{aligned} u &= \theta, & u' &= \Theta, \\ t &= \lambda-\lambda_o, & t' &= \pi - \Lambda \\ e &= \theta_o . \end{aligned}$$

The results are

$$P_n^{\mu}(\cos\theta)\cos(\lambda-\lambda_0) = \sum_{m=0}^{n} A_{m\mu} P_n^{m}(\cos\textcircled{H})\cos m(\pi-\Lambda)$$
$$P_n^{\mu}(\cos\theta)\sin(\lambda-\lambda_0) = \sum_{m=0}^{n} B_{m\mu} P_n^{m}(\cos\textcircled{H})\sin m(\pi-\Lambda) \quad (8)$$

These formulae can be used for the transformation of the wind velocity into the gm coordinates in the general case.

If we take $\mu = 0$ (for non-periodic winds) we have

$$P_n^{0}(\cos\theta) = \sum_{m=0}^{n} P_n^{m}(c)\, P_n^{m}(\cos\textcircled{H})\cos m(\pi-\Lambda)$$

Taking $n = 1$ for example,

$$P_1^{0}(\cos\theta) = P_1^{0}(c)\, P_1^{0}(\cos\textcircled{H}) + P_1^{1}(c)\, P_1^{1}(\cos\textcircled{H})\cos(\pi-\Lambda)$$

i.e.,

$$\cos\theta = \cos\theta_0\cos\textcircled{H} - \sin\theta_0\sin\textcircled{H}\cos\Lambda$$

and using the relation

$$\sin\theta = (1 - \cos^2\theta)^{\frac{1}{2}}$$

we have the expression of $2\sin\theta\cos\theta$ in the gm coordinates. This form will be used as an example for the longitudinal distribution of the meridional component of non-periodic winds.

5. CONDUCTIVITY AND WIND PROFILES

In order to solve the basic equation (4), we need to have the numerical values of the coefficients A, B, C and D,

where A, B and C are functions of conductivity only, whereas D includes the wind velocity $\vec{V}$.

The distribution and variation of conductivity are obtained as follows: Atmospheric parameters, such as temperature, density, molecular weight and so on, are taken from the U. S. Standard Atmosphere (1962). The distribution of electron density with height and latitude at noon are estimated, for a period of high sunspot activity, from the results of recent radio and rocket observations. By using these atmospheric and ionospheric models, the height-integrated conductivities K_{xx}, K_{yy} and K_{xy} are calculated and the results are shown in Fig. 2. Since we do not yet have any detailed information about the time-dependent structure of the lower ionosphere, especially about the height distribution of electron density, the following formula for the variation of conductivity (Chapman and Bartels, 1940) is used:

$$K = K_o \left(1 + \sum_{s=1}^{3} k_s \cos^s \chi\right)$$

where χ is the zenith distance of the sun. The values of the coefficients k_s are estimated as follows, by taking into account the latitudinal distribution of noon conductivity and the height distribution of electron density observed by rockets at night (e.g., Bourdeau, 1963):

$$k_1 = 3.0, \quad k_2 = 3.0, \quad k_3 = 0.9$$

This gives the night-time conductivity of about one fifties of the daytime one at middle and low latitudes.

Although we have now so many results of observations of winds at heights lower than 100 km (see for example, a review by Murgatroyd, 1957), very few are known about the wind structure in regions higher than 100 km. This seems to be due to the reason that the method of wind measurements taken at the lower atmosphere cannot be applicable to the upper atmosphere because of low density, and that the wind structure at heights of interest (say, around 120 km) is very complicated perhaps because of the interaction of the neutral and ionized components of atmospheric gases. Thus, unfortunately, we cannot as yet set any reliable profiles of non-periodic winds. We shall employ here, therefore, only hypothetical wind profiles as shown in Table 1 and illustrated in Fig. 3, which might be deduced from informations about ionospheric drifts and also wind structures in the lower atmosphere. Cases (AZ) and (AM) are chosen to be similar to those adopted by van Sabben (1962) for the convenience of comparison.

Table 1. Supposed profiles of non-periodic winds.

	Meridional (Southward positive)
Case (AM)	$V_x = - V_o \sin (2\theta)$
Case (BM)	$V_x = - V_o \sin (4\theta)$
	Zonal (Eastward positive)
Case (AZ)	$V_y = - V_o (2.7 \sin\theta - 4.0 \sin^3\theta)$
Case (BZ)	$V_y = - V_o \sin (4\theta)$

Note: θ is co-latitude.

V_o is taken to be 10 m/sec in this paper.

6. CALCULATION OF THE DYNAMO FIELD

In the case where the gg coordinates are taken, the velocity distribution can be used in its original form, and we have the following expressions for the dynamo fields:

$$E_{dx} = -C\ F\ V_y$$

$$E_{dy} = C\ F\ V_x$$

where

$$C = 2\ M/a^3,$$

$$F = \cos\theta_o \cos\theta + \sin\theta_o \sin\theta \cos(\lambda - \lambda_o)$$

which has been obtained in section 4.2.

In the case where the gm coordinates are taken, the velocity distribution must be transformed. This transformation can be made by using the method presented in section 4.3., and we have the following results:

$$\left.\begin{aligned} E_{dx} &= V_o\, C\, F_1\, F_5 \\ E_{dy} &= -\, V_o\, C\, F_3\, F_5 \end{aligned}\right\} \quad \text{for Case (AZ)}$$

$$\left.\begin{aligned} E_{dx} &= 4\, V_o\, C\, F_1\, F_2\, F_4 \\ E_{dy} &= -\, 4\, V_o\, C\, F_2\, F_3\, F_4 \end{aligned}\right\} \quad \text{for Case (BZ)}$$

$$\left.\begin{aligned} E_{dx} &= -\, 2\, V_o\, C\, F_2\, F_3 \\ E_{dy} &= -\, 2\, V_o\, C\, F_1\, F_2 \end{aligned}\right\} \quad \text{for Case (AM)}$$

$$\left.\begin{aligned} E_{dx} &= -\, 4\, V_o\, C\, F_2\, F_3\, F_4 \\ E_{dy} &= -\, 4\, V_o\, C\, F_1\, F_2\, F_4 \end{aligned}\right\} \quad \text{for Case (BM)}$$

where

$$F_1 = \cos\textcircled{H}(\cos\theta_o \sin\textcircled{H} + \sin\theta_o \cos\textcircled{H} \cos\Lambda)$$

$$F_2 = \cos\theta_o \cos\textcircled{H} - \sin\theta_o \sin\textcircled{H} \cos\Lambda$$

$$F_3 = \sin\theta_o \cos\textcircled{H} \sin\Lambda$$

$$F_4 = 2\,(F_2)^2 - 1$$

$$F_5 = 4\,(F_2)^2 - 1.3$$

7. METHOD OF NUMERICAL SOLUTIONS

There are two methods for numerical solutions of eq. (4). One deals with the equation in its original form, and the

other is to modify the original equation to ordinary differential equations by expanding the potential S (unknown) into Fourier series. It seems that the latter is, in general, more easy to obtain solutions than the former. In this case, however, we must interrupt the series at the first several terms for practical calculations, so that significant error might be introduced. For this reason, we adopt here the former method, that is, eq. (4) has been modified to a finite-difference form and solved by Liebmann's iteration method on a IBM system/360 computer. We do not want to describe details for the method employed, but give only essential points below.

Returning to eq. (4), if we use the relation

$$t = ut + \lambda$$

among the local time (t), the universal time (UT) and the longitude (λ), the coefficients A, B, C and D are regarded as functions of space coordinates (θ, λ) only, at a particular UT. Thus, the numerical integration can be made only for space coordinates, and we have a set of solutions for different UT's. The mesh has been taken to be 2.5° for θ, and 7.5° for λ, and solutions have, in most cases, been converged within limits of error for several minutes. This would be due to the reason that our basic equation is, fortunately, of elliptic type.

Concerning the polar boundary condition, we have tried the case in which all the boundary values are taken to be zero, and found that no significant difference is seen in solution and also in time of convergence, as compared with the case in which the boundary values estimated by Taylor expansion are used. This is due to the fact that the boundary values close to the north pole are very small, because we have assumed that S = 0 at the pole.

8. RESULTS AND DISCUSSIONS

The distributions of the electrostatic potential (S) and the current functions (R) at UT = 0^h calculated for different wind profiles, as is shown in Table 1, are illustrated in Figs. 4A to 4D. These results are obtained by using the geomagnetic coordinates and by taking V_o = 10 m/sec. It is found from these figures that: 1) For all of these four cases, current vortices are produced and their patterns are similar to those of Sq, namely, they have counter-clockwise flow of currents and much enhanced intensity in daytime. 2) The intensities of daytime current cortices are

6,000 amperes for Case (AZ)

16,000 amperes for Case (AM)

4,000 amperes for Case (BZ)

8,000 amperes for Case (BM)

so that the meridional wind is more effective in producing current systems than the zonal one, and these intensities are about one tenth of those of the Sq vortices. 3) In most cases clockwise and weak current vortices are produced in high latitudes.

The cases where the zonal and meridional winds are combined are also calculated and we have Fig. 5 for R. The intensity of main current vortices is 20,000 amperes for Case (A) and 10,000 amperes for Case (B). It is seen that the center of current vortices is much closer to the equator for Case (A) than for Case (B), and it may therefore be said that the distribution of conductivity had a leading effect for Case (A) in determining the position of current vortices, whereas the distribution of wind velocity played more important role for Case (B). In this connection, the Sq like current systems obtained by van Sabben (1962) might be much distorted, if the latitudinal and local time variations of conductivity are taken into account, even in daylight hours.

In order to see the effect of different coordinate systems on the results, similar calculations are made by using the geo-

graphic coordinates for Case (AM) and Case (BZ), as an example, and we have the results as shown in Fig. 6. Comparison of Figs. 4 and 6 for corresponding cases shows that no remarkable difference can be seen in the intensity and also in the general pattern of current systems, though there are slight differences in the shape of current vortices.

All the figures presented above are the results obtained for UT = 0^h. An example for different UT's is shown in Fig. 7, where ⊙ shows the position of noon. It is found that both the shape and the intensity of current systems are changing with UT, and this may correspond to the UT variation in the Sq field. In order to see this point more clearly, we separate these changing current systems in such a way as follows:

First, if we fix the local time and average over UT's, then a current system as shown in Fig. 8A is obtained. Since this system depends only on local time, it may be called the local time part and this part would have a main contribution to the Sq current system.

Next, if we fix the longitude and average over UT's and subtract the non-periodic component of R, because this part has already been included in the local time part, we have the

results as shown in Fig. 8B. This system depends only on longitude and therefore it may be called the longitudinal part. Since this part gives a longitudinal inequality in current systems, it is expected that the maximum intensity of current vortices, and therefore the madimum magnetic effect, occurs around Λ (geomagnetic longitude) = 0°, i.e., the north and south American zone, and the minimum around $\Lambda = 180^{\circ}$, i.e., the Asia and Oceania zone. This tendency is in good agreement with that as seen in the Sq field (see for example, Price and Wilkins, 1963; Matsushita and Maeda, 1965) and also in the equatorial electrojet (Sugiura and Cain, 1966). It may therefore be said that the longitudinal inequality in the Sq field is caused partly by the incoincidence of the Earth's rotational and magnetic axes, and partly by the distribution of ionospheric conductivity due perhaps to the longitudinal inequality in the geomagnetic field intensity.

Finally, if we take the non-periodic part at each UT and subtract the average over UT's, we have the universal time part depending only on universal time as is shown in Fig. 8C. It is expected from this figure that the current vortices would be most enhanced around UT = 20^{h} and least enhanced around UT = 9^{h}. Note, however, that these three parts cannot be indepen-

dent because of the relation, $t = UT + \Lambda$, where t is geomagnetic local time and UT is geomagnetic universal time defined by refering to the meridian $\Lambda = 0^{\circ}$, because the geomagnetic coordinates are taken.

9. CONCLUSIONS

From the foregoing detailed calculations of electric currents induced by non-periodic winds in the ionosphere, when the incoincidence of the rotational and magnetic axes of the Earth is taken into account, the following conclusions may be drawn:

1) Sq-like current systems can be produced by non-periodic components of ionospheric winds as an effect of the axes incoincidence, even for the two dimensional case of the dynamo theory.

2) When a typical wind velocity of 10 m/sec is taken, the induced current intensity is about ten thousand volts, being about one tenth of that of the Sq field.

3) Of the two components of non-periodic winds, the meridional component is more (two or three times) effective in producing current systems.

4) The position of main current vortices is controlled

by the distributions of ionospheric conductivity and of wind velocity, and the degree of incluence of these two is different for different wind profiles.

5) No remarkable difference can be seen in the results obtained by using different (geographic and geomagnetic) coordinate systems.

6) The intensity and the pattern of current systems change with longitude and universal time. The maximum intensity occurs around 0^{o} in geomagnetic longitude (the north and south American zone) and 20^{h} in geomagnetic universal time, and the minimum around 180^{o} (the Asia and Oceania zone) and 9^{h}, respectively.

Since the intensity of current vortices is proportional to the velocity of winds, it would be said that the effect of axes incoincidence cannot be negligible when much stronger winds exist.

ACKNOWLEDGEMENTS

One of us (H. Maeda) is very much obliged to Dr. Robert Jastrow, Director of the Institute for Space Studies, for his interest in and support of this work.

He is also expressing his appreciation to the National

Academy of Sciences - National Research Council for a Senior Research Associateship.

REFERENCES

Bourdeau, R. E., Ionospheric research from space vehicles, Space Sci. Rev., 1, 683-728, 1963.

Chapman, S., and J. Bartels, Geomagnetism, Oxford University Press, p. 771, 1940.

Chapman, S., The electrical conductivity of the ionosphere; a Review, Nuovo Cimento, 4, Serie X, Suppl. No. 4, 1-28, 1956.

DeWitt, R. N., and S.-I. Akasofu, Dynamo action in the ionosphere and motions of the magnetospheric plasma, I. Symmetric dynamo action, Planet. Space Sci., 12, 1147-1156, 1964.

Gupta, J. C., Relative importance of solar radiation and gravitational tide in causing geomagnetic variations, J. Geophys. Res., 72, 1583-1589, 1967.

Jones, W. L., Energetics of the solar semidiurnal tide in the atmosphere, AFCRL-63-690, 1963.

Kato, S., Prevailing wind in the ionosphere and geomagnetic Sq variations, J. Geomag. Geoelect., 9, 215-217, 1957.

Maeda, H., Generalized dynamo mechanism in the upper atmosphere, J. Geomag. Geoelect., 18, 173-182, 1966.

Maeda, K., and H. Matsumoto, Paper presented at the 1962 Fall meeting of the Society of Terrestrial Magnetism and Electricity, Japan, not published.

Matsushita, S., and H. Maeda, On the geomagnetic solar quiet daily variation field during the IGY, J. Geophys. Res., 70, 2535-2558, 1965.

Murgatroyd, R. J., Winds and temperatures between 20 km and 100 km; a Review, Quart. J. Roy. Meteorol. Soc., 83, 417-458, 1957.

Price, A. T., and G. A. Wilkins, New methods for the analysis of geomagnetic fields and their application to the Sq field of 1932-33, Phil. Trans. Roy. Soc. London, A 259, 31-98, 1963.

Schmidt, A., Tafeln der normierten Kugelfunktionen, Gotha, Engelhard-Reyher Verlag, 1935.

Sugiura, M., and J. C. Cain, A model equatorial electrojet, J. Geophys. Res., 71, 1869-1877, 1966.

U. S. Standard Atmosphere, 1962, U. S. Government Printing Office, Washington, D. C., 1962.

van Sabben, D., Ionospheric current systems caused by non-periodic winds, J. Atmos. Terr. Phys., 24, 959-974, 1962.

FIGURE CAPTIONS

Fig. 1. Showing relation of any two spherical coordinate systems, (u,t) and (u',t').

Fig. 2. Latitudinal distribution of height-integrated noon conductivities, K_{xx}, K_{yy} and K_{xy}.

Fig. 3. Illustration of the four profiles of non-periodic winds as is shown in Table 1.

Fig. 4A. Distribution of the electrostatic potential (S) and the current function (R) for Case (AZ), where electric currents flow in the direction indicated by arrows along the equal R (strem) lines.

Fig. 4B. Distribution of S and R for Case (AM).

Fig. 4C. Distribution of S and R for Case (BZ).

Fig. 4D. Distribution of S and R for Case (BM).

Fig. 5. Distribution of the current function (R) for combined winds; Case (A) is obtained by a combination of profiles (AZ) and (AM), and Case (B) by a combination of profiles (BZ) and (BM).

Fig. 6. Distribution of the current function (R) calculated by using the geographic coordinates for wind profiles (AM) and (BZ).

Fig. 7. Variation of current systems with universal time, where ⊙ shows the position of noon.

Fig. 8A. Local time part of the current systems as shown in Fig. 7.

Fig. 8B. Longitudinal part of the current systems as shown in Fig. 7.

Fig. 8C. Universal time part of the current systems as shown in Fig. 7.

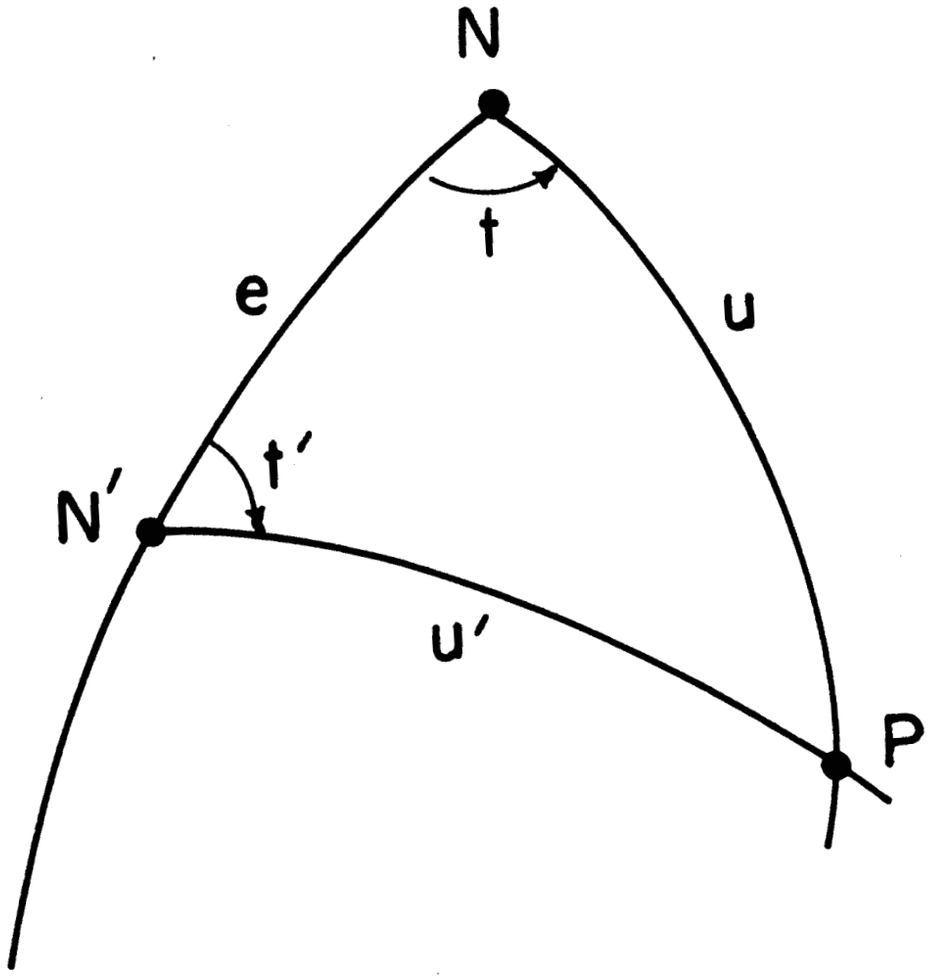

Fig. 1.

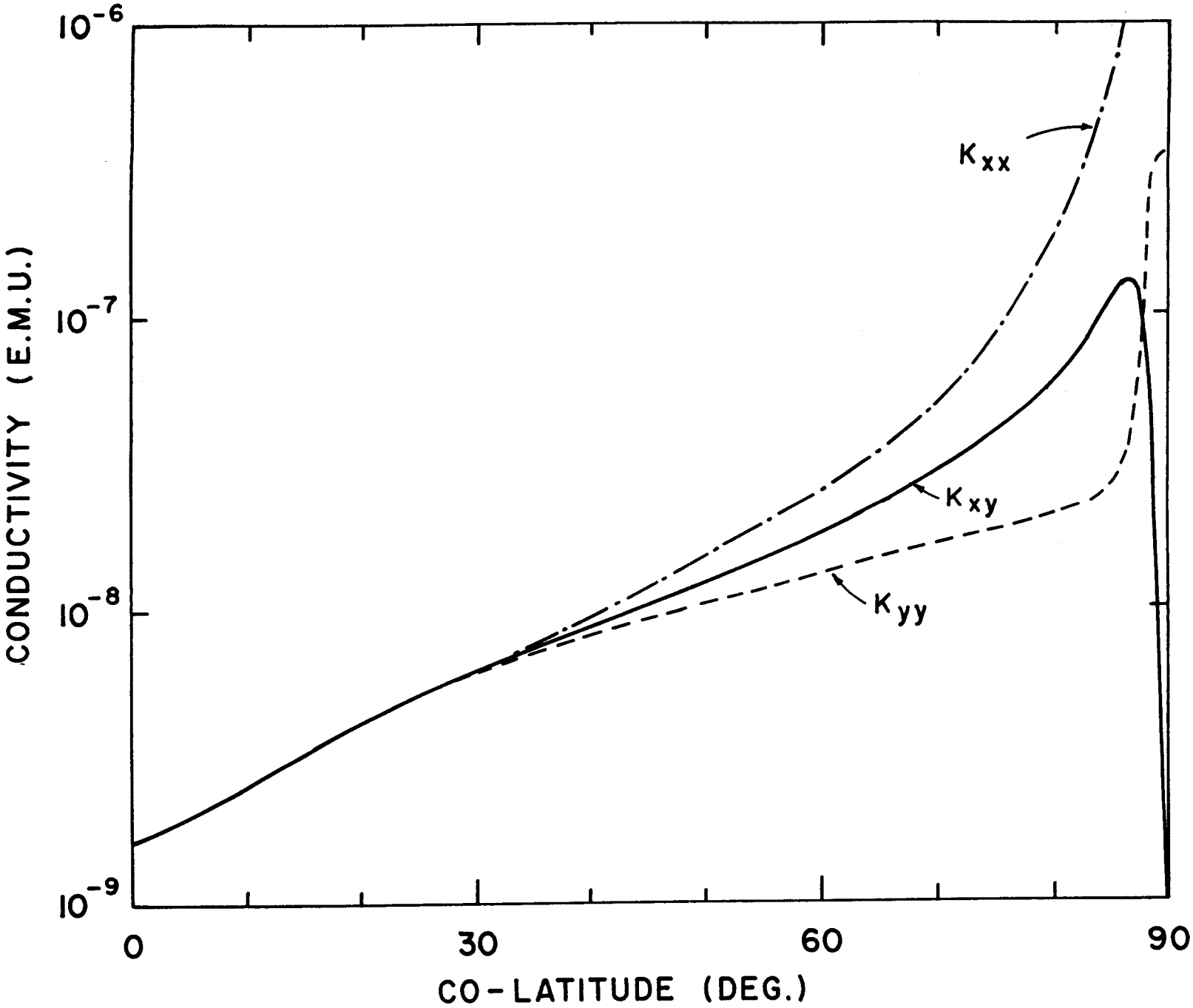
10^{-6}
10^{-7}
10^{-8}
10^{-9}
CONDUCTIVITY (E.M.U.)
K_{xx}
K_{xy}
K_{yy}
0
30
60
90
CO-LATITUDE (DEG.)

Fig. 2.

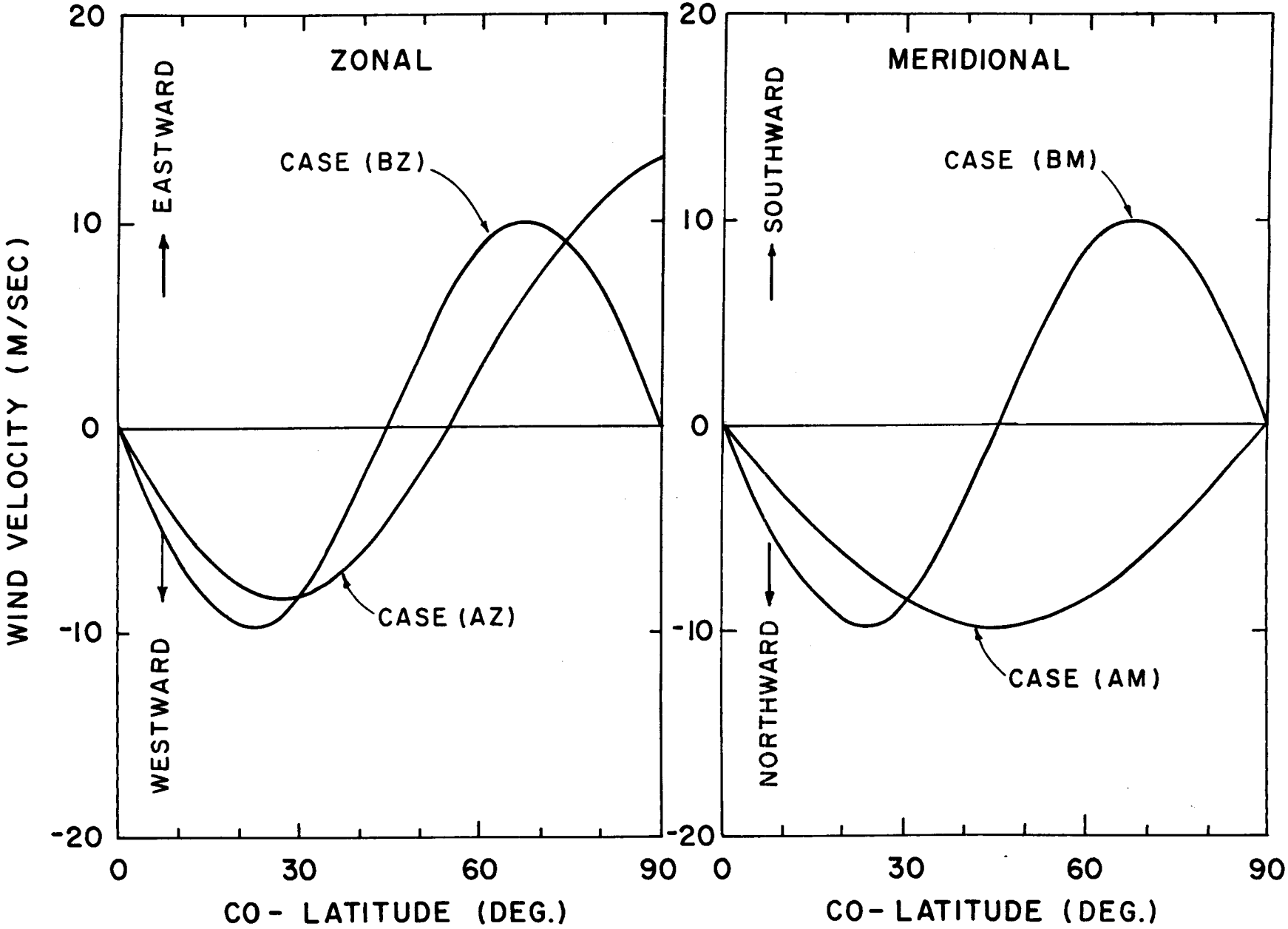
ZONAL
MERIDIONAL
EASTWARD
WESTWARD
SOUTHWARD
NORTHWARD
CASE (BZ)
CASE (AZ)
CASE (BM)
CASE (AM)
WIND VELOCITY (M/SEC)
CO- LATITUDE (DEG.)
CO- LATITUDE (DEG.)
20
10
0
-10
-20
0
30
60
90

Fig. 3.

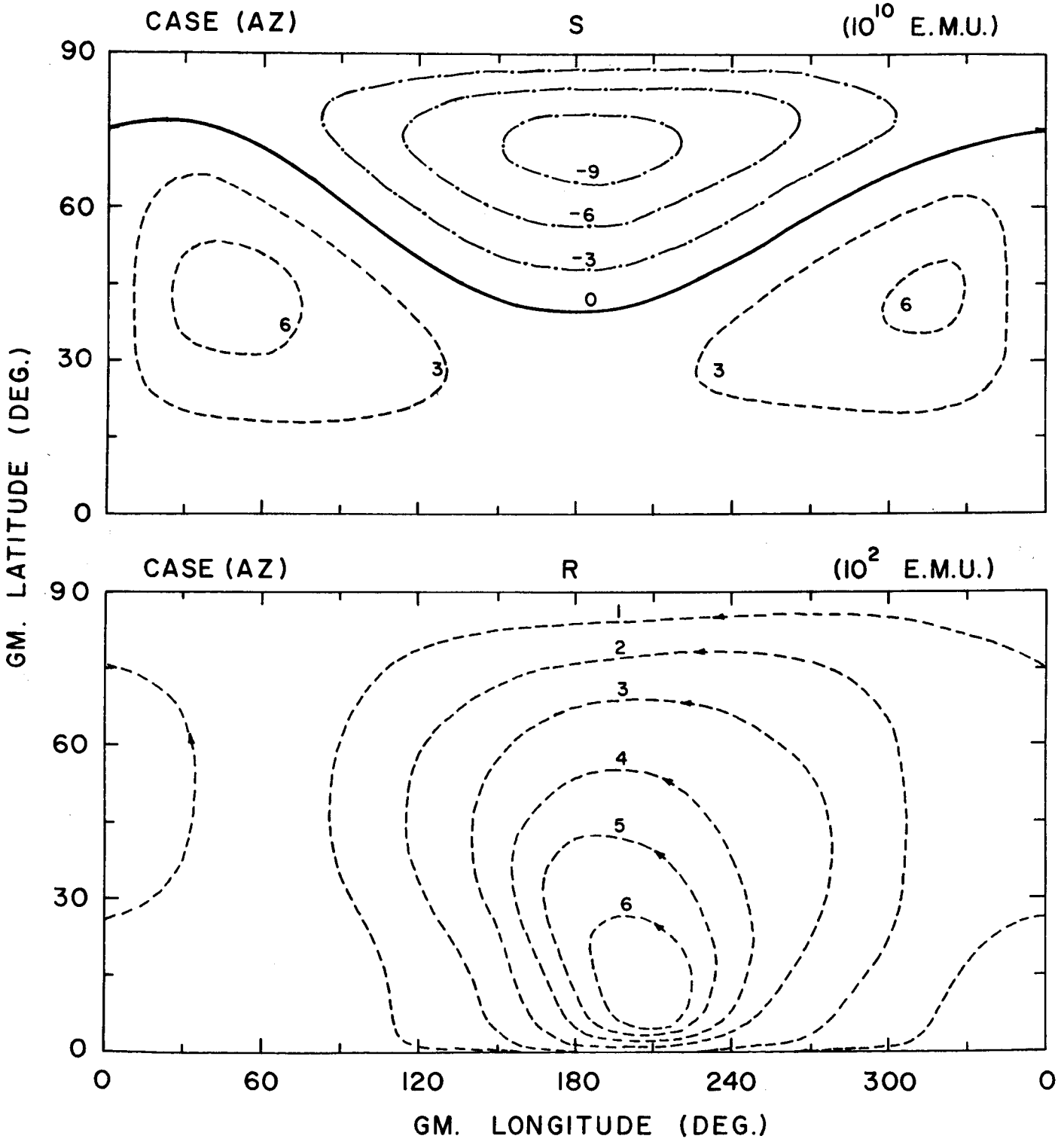
CASE (AZ)
S
(10^10 E.M.U.)
90
60
30
0
-9
-6
-3
0
6
3
6
3
CASE (AZ)
R
(10^2 E.M.U.)
90
60
30
0
1
2
3
4
5
6
0
60
120
180
240
300
0
GM. LATITUDE (DEG.)
GM. LONGITUDE (DEG.)

Fig. 4A.

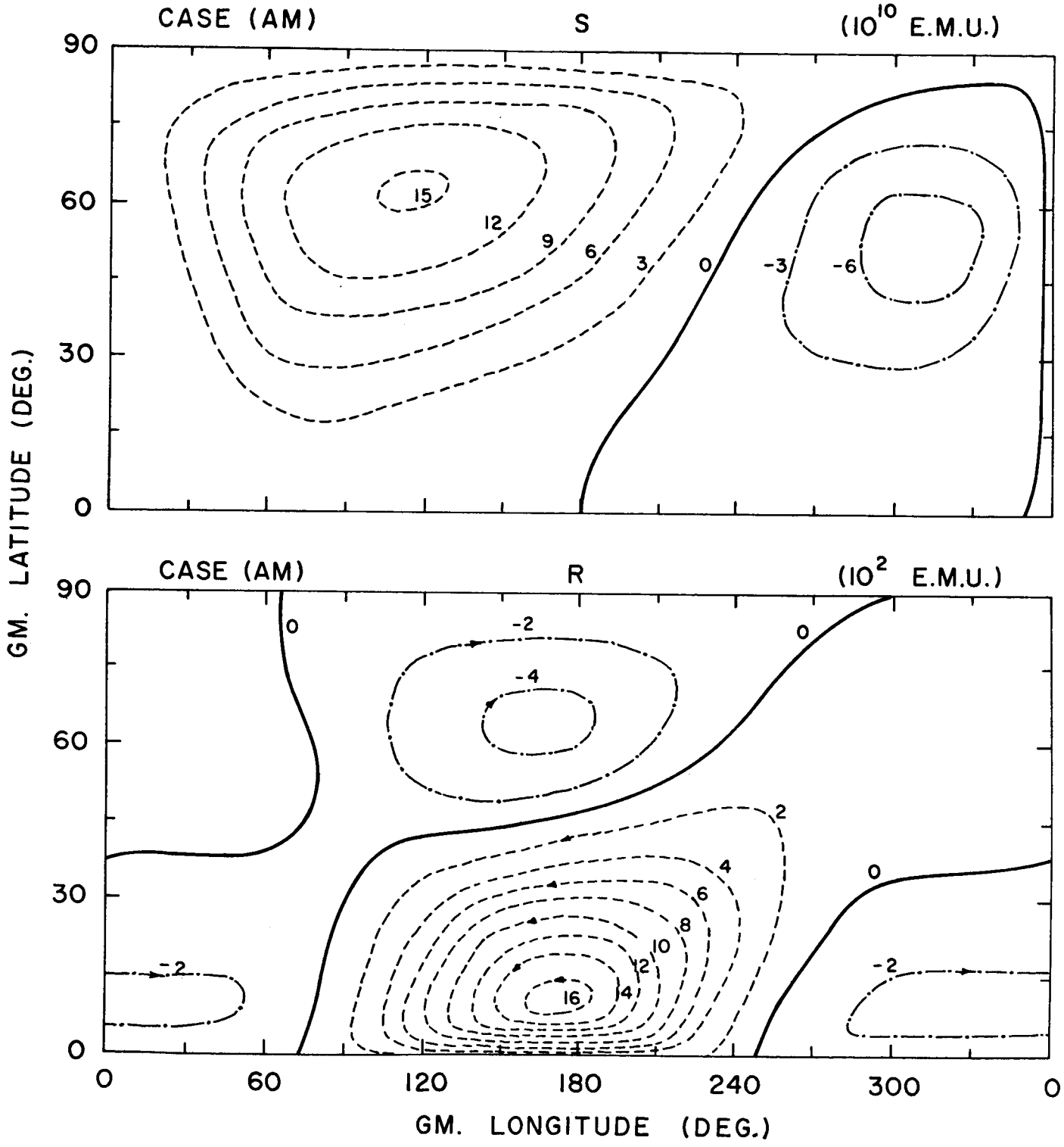
CASE (AM)
S
(10^10 E.M.U.)
90
60
30
0
15
12
9
6
3
0
-3
-6
CASE (AM)
R
(10^2 E.M.U.)
90
60
30
0
0
-2
-4
0
2
4
6
8
10
12
14
16
0
-2
-2
0
60
120
180
240
300
0
GM. LONGITUDE (DEG.)
GM. LATITUDE (DEG.)

Fig. 4B.

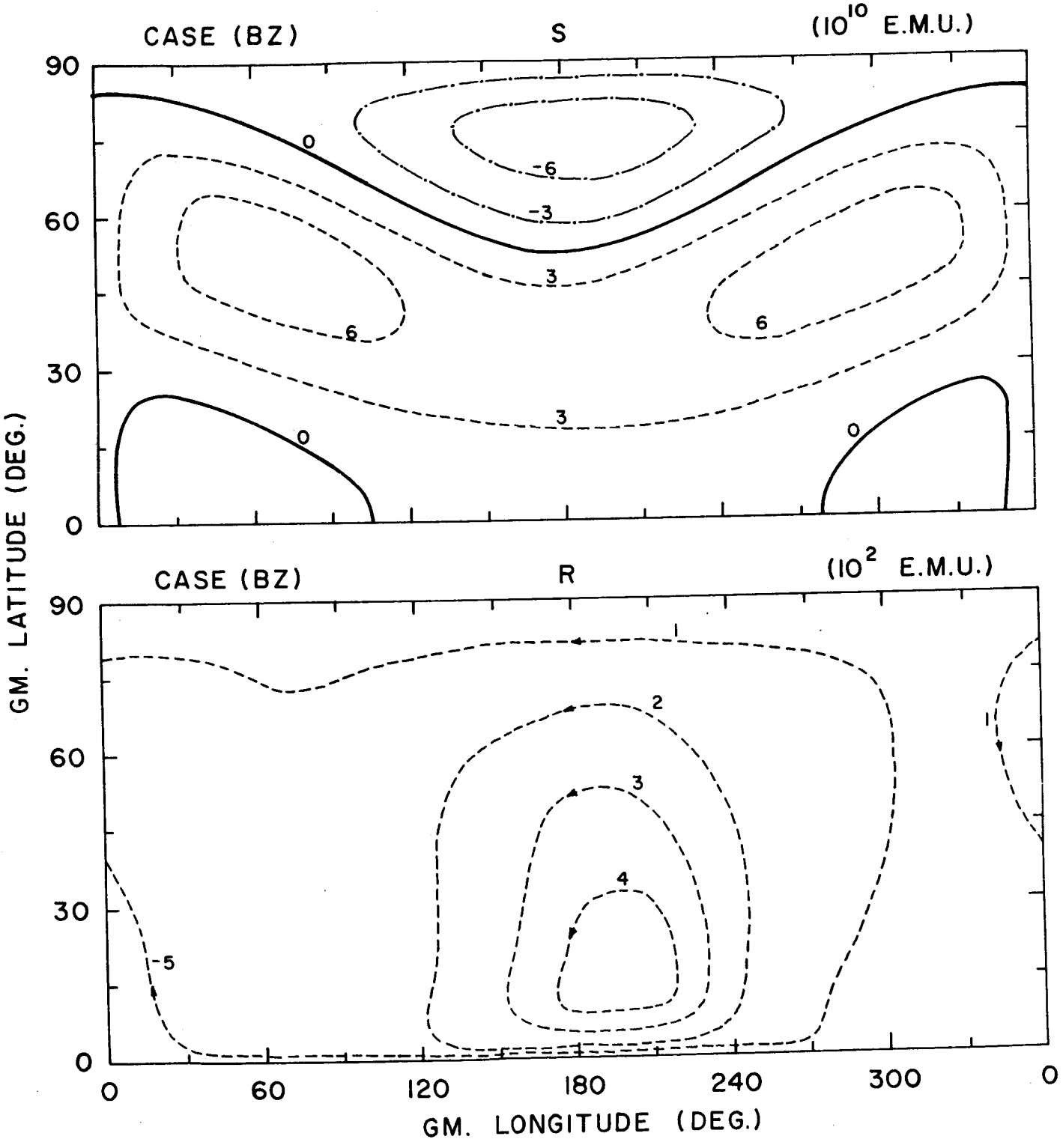
CASE (BZ)
S
(10^10 E.M.U.)
90
60
30
0
0
-6
-3
3
6
6
3
0
0
GM. LATITUDE (DEG.)
CASE (BZ)
R
(10^2 E.M.U.)
90
60
30
0
2
3
4
-5
1
0
60
120
180
240
300
0
GM. LONGITUDE (DEG.)

Fig. 4C.

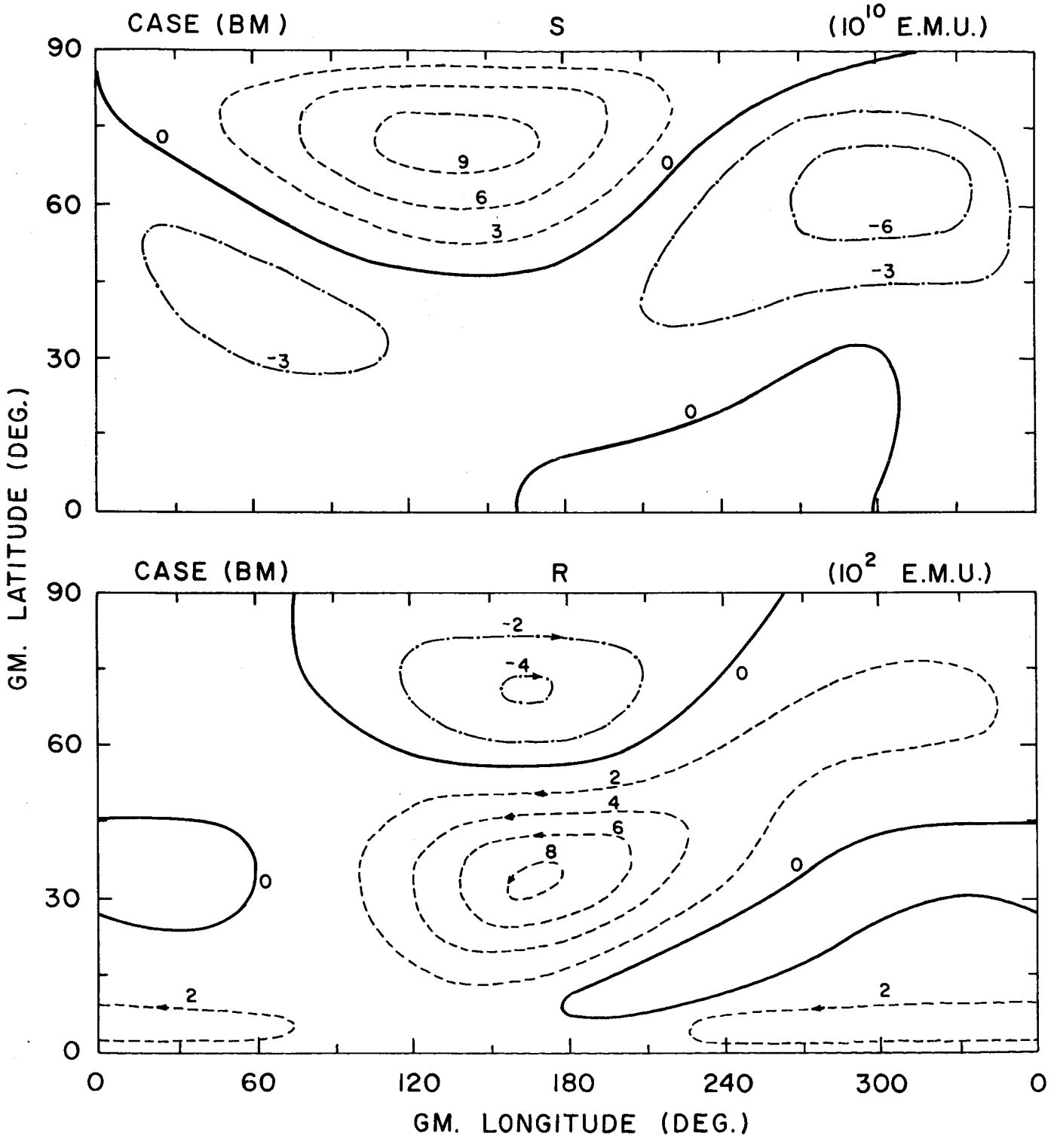
CASE (BM)
S
(10^10 E.M.U.)
90
60
30
0
0
9
6
3
0
-6
-3
-3
0
CASE (BM)
R
(10^2 E.M.U.)
-2
-4
0
2
4
6
8
0
0
2
2
GM. LATITUDE (DEG.)
0
60
120
180
240
300
0
GM. LONGITUDE (DEG.)

Fig. 4D.

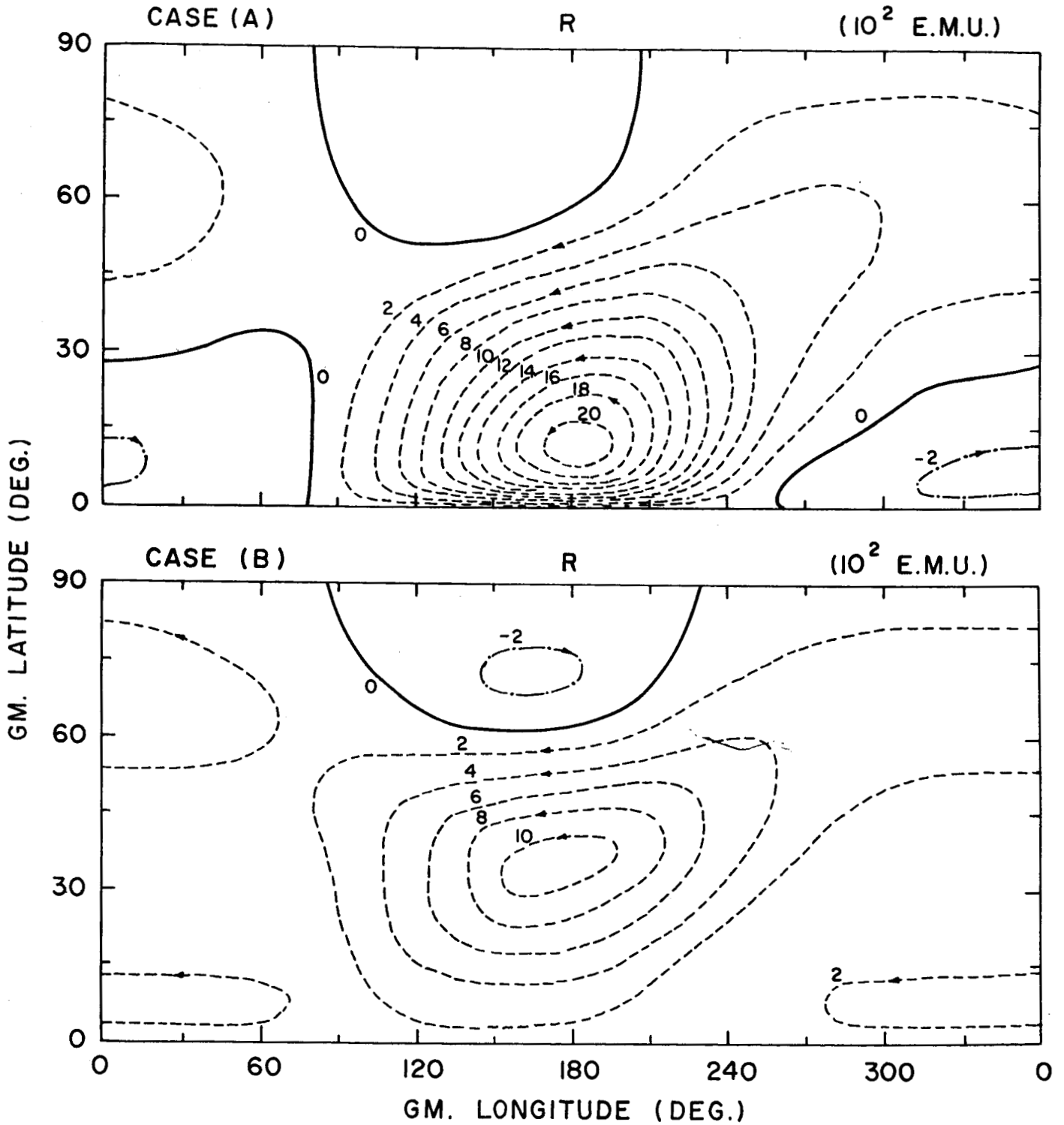
CASE (A)
R
(10² E.M.U.)
90
60
30
0
0
2
4
6
8
10
12
14
16
18
20
-2
CASE (B)
R
(10² E.M.U.)
-2
2
4
6
8
10
GM. LATITUDE (DEG.)
0
60
120
180
240
300
0
GM. LONGITUDE (DEG.)

Fig. 5.

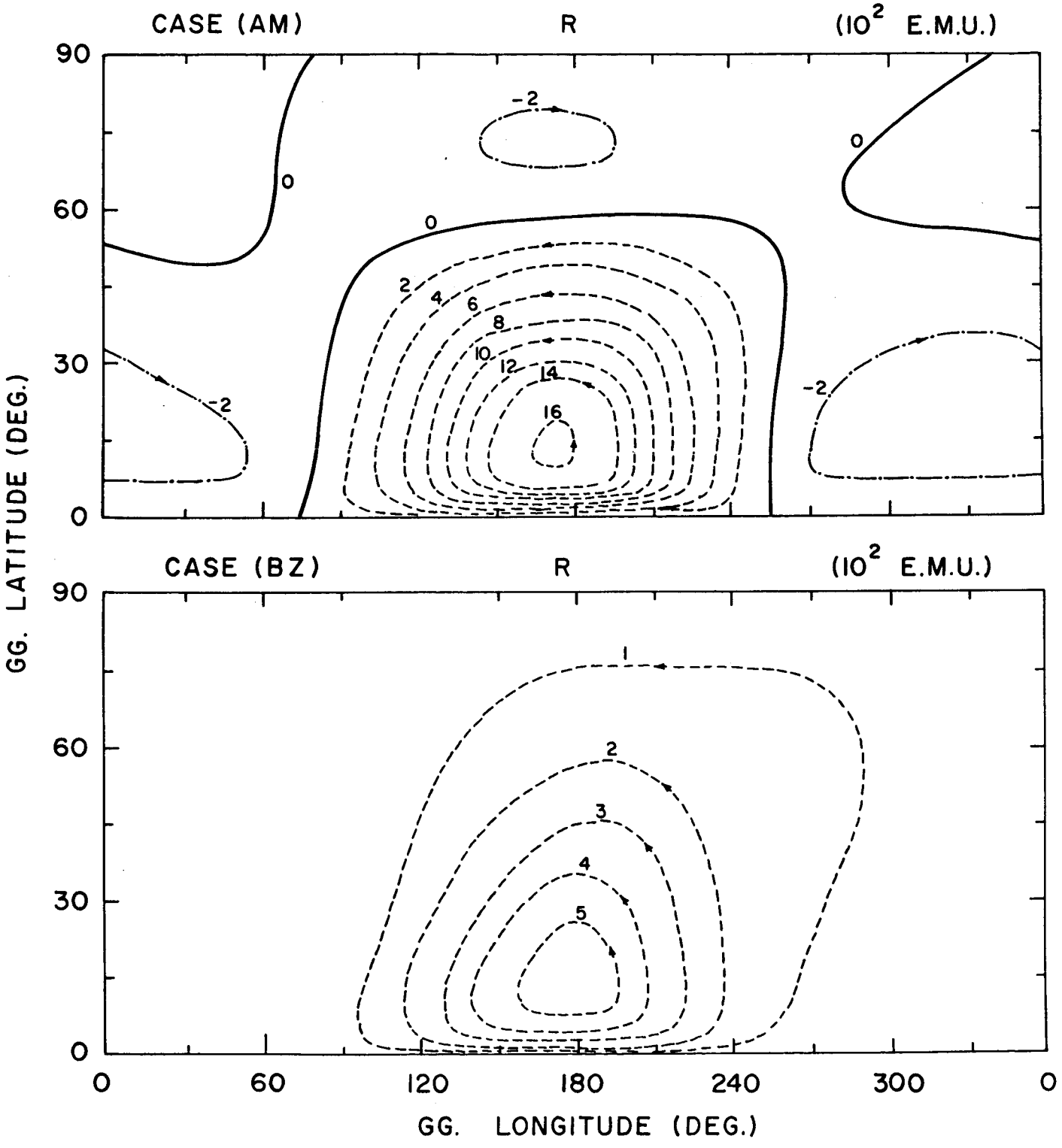
CASE (AM)
R
(10² E.M.U.)
90
60
30
0
-2
0
0
2
4
6
8
10
12
14
16
-2
0
-2
CASE (BZ)
R
(10² E.M.U.)
90
60
30
0
1
2
3
4
5
0
60
120
180
240
300
0
GG. LATITUDE (DEG.)
GG. LONGITUDE (DEG.)

Fig. 6.

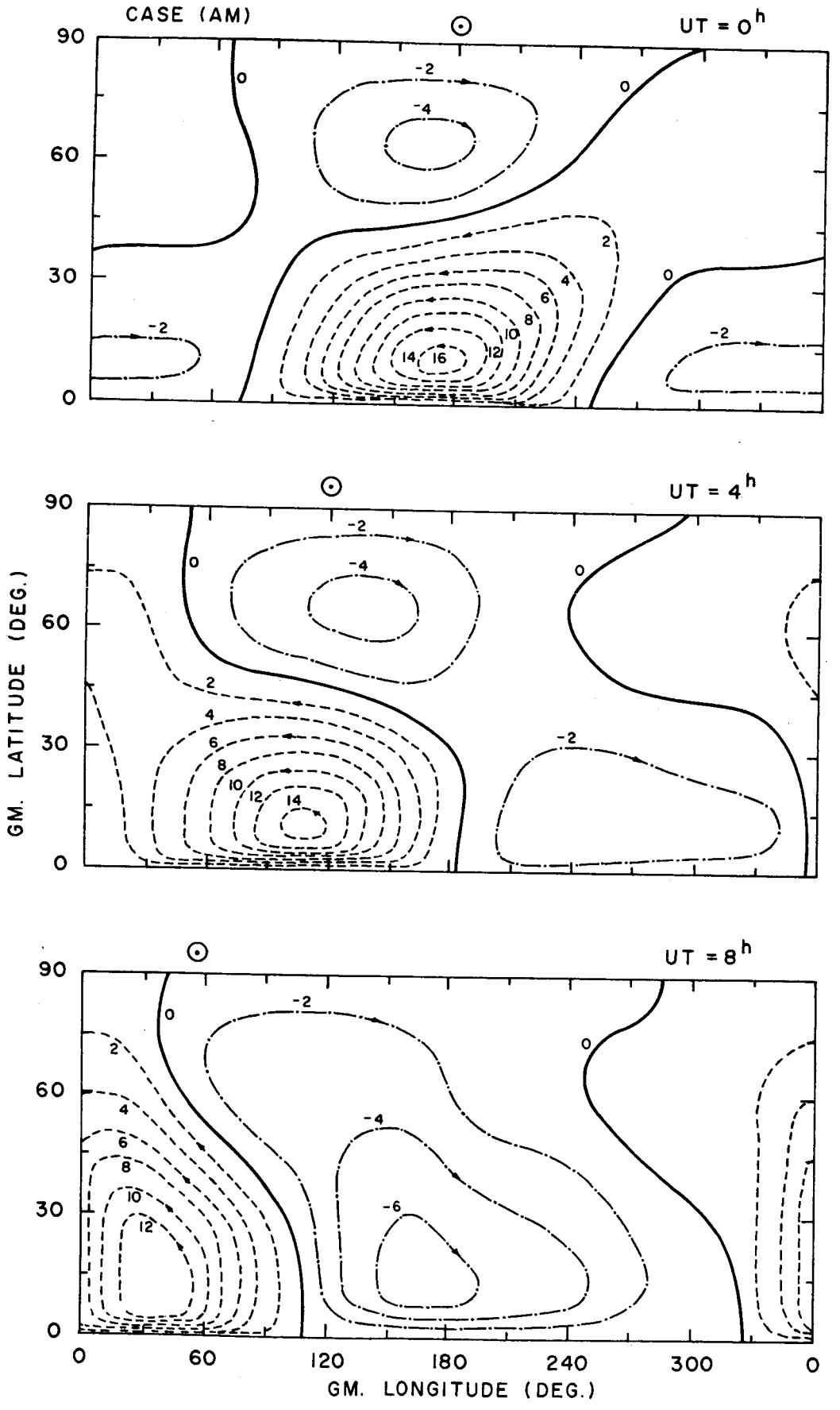
CASE (AM)
UT = 0h
UT = 4h
UT = 8h
90
60
30
0
GM. LATITUDE (DEG.)
0
60
120
180
240
300
0
GM. LONGITUDE (DEG.)

Fig. 7.

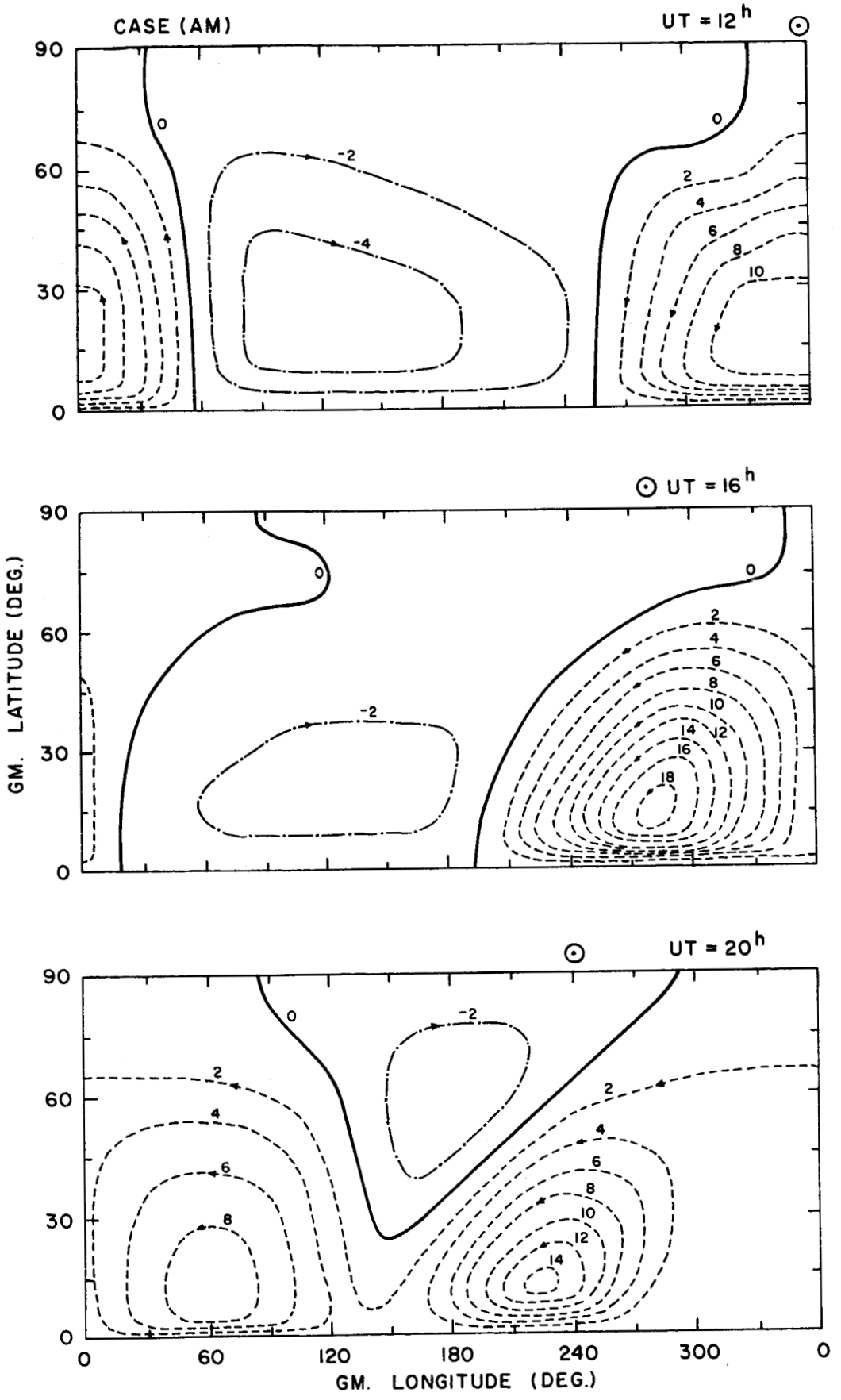

Fig. 7. (continued)

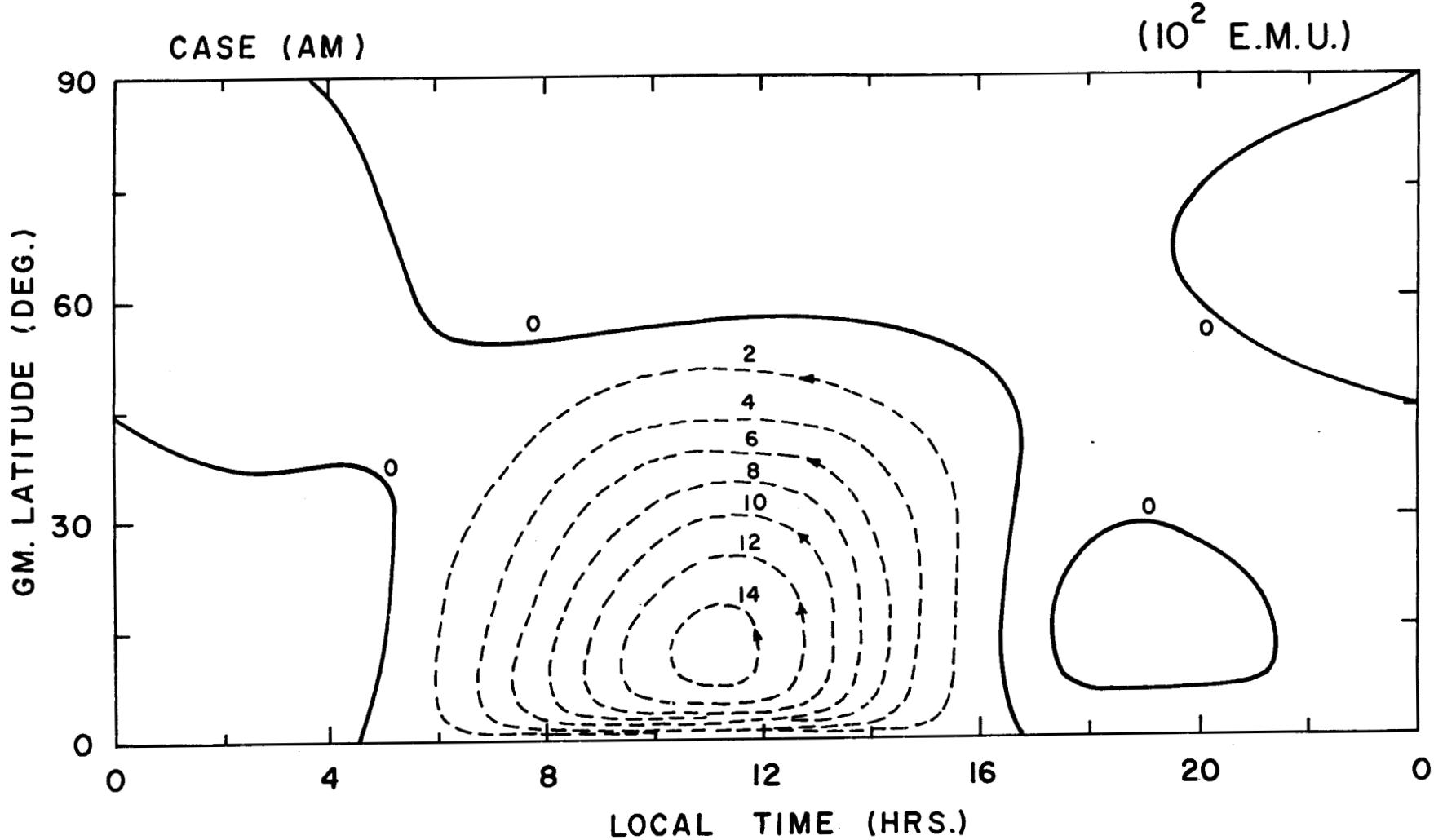
CASE (AM)
(10² E.M.U.)
90
60
30
0
GM. LATITUDE (DEG.)
0
4
8
12
16
20
0
LOCAL TIME (HRS.)
0
0
0
2
4
6
8
10
12
14

Fig. 8A.

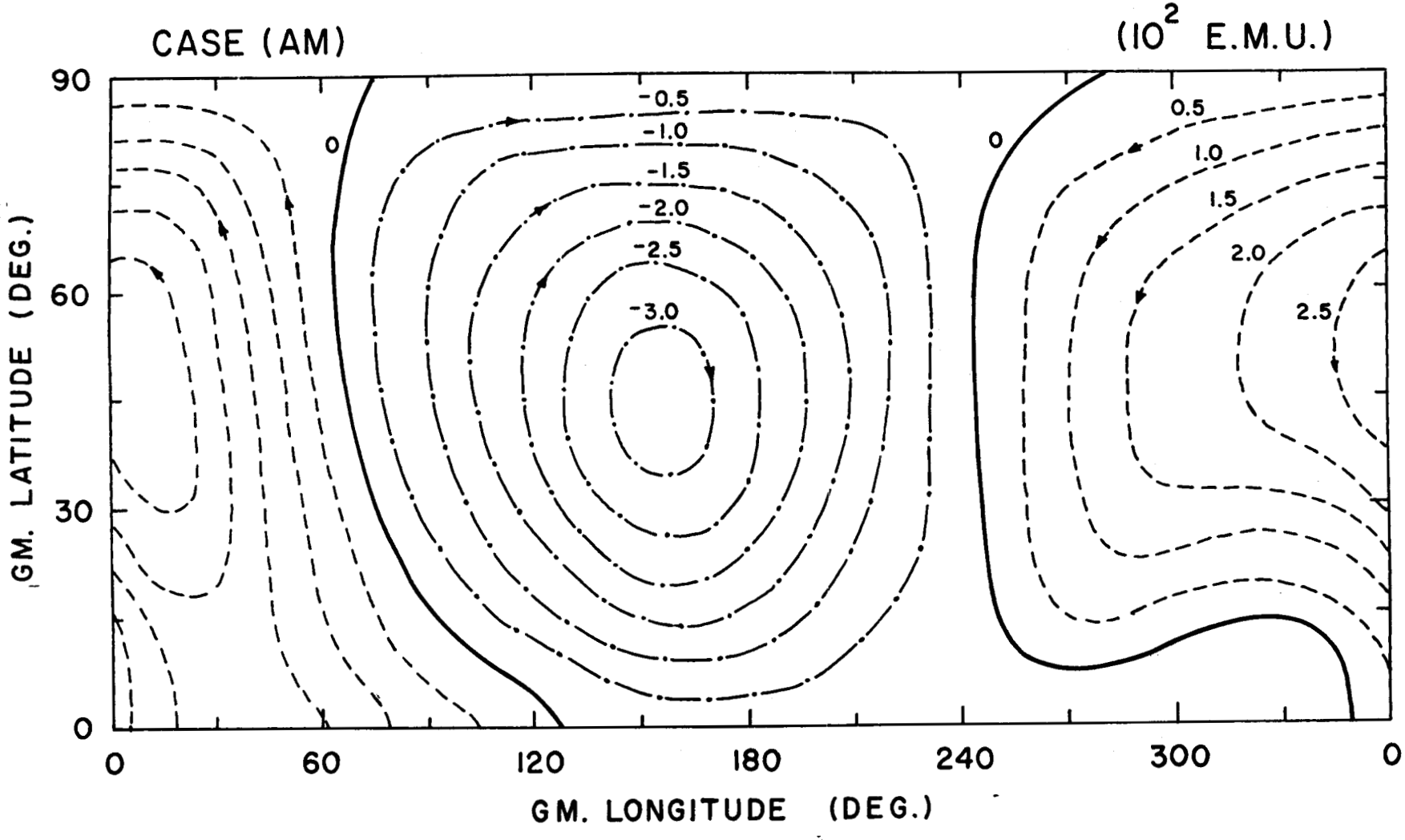
CASE (AM)
(10² E.M.U.)
90
60
30
0
GM. LATITUDE (DEG.)
0
60
120
180
240
300
0
GM. LONGITUDE (DEG.)
-0.5
-1.0
-1.5
-2.0
-2.5
-3.0
0
0
0.5
1.0
1.5
2.0
2.5

Fig. 8B.

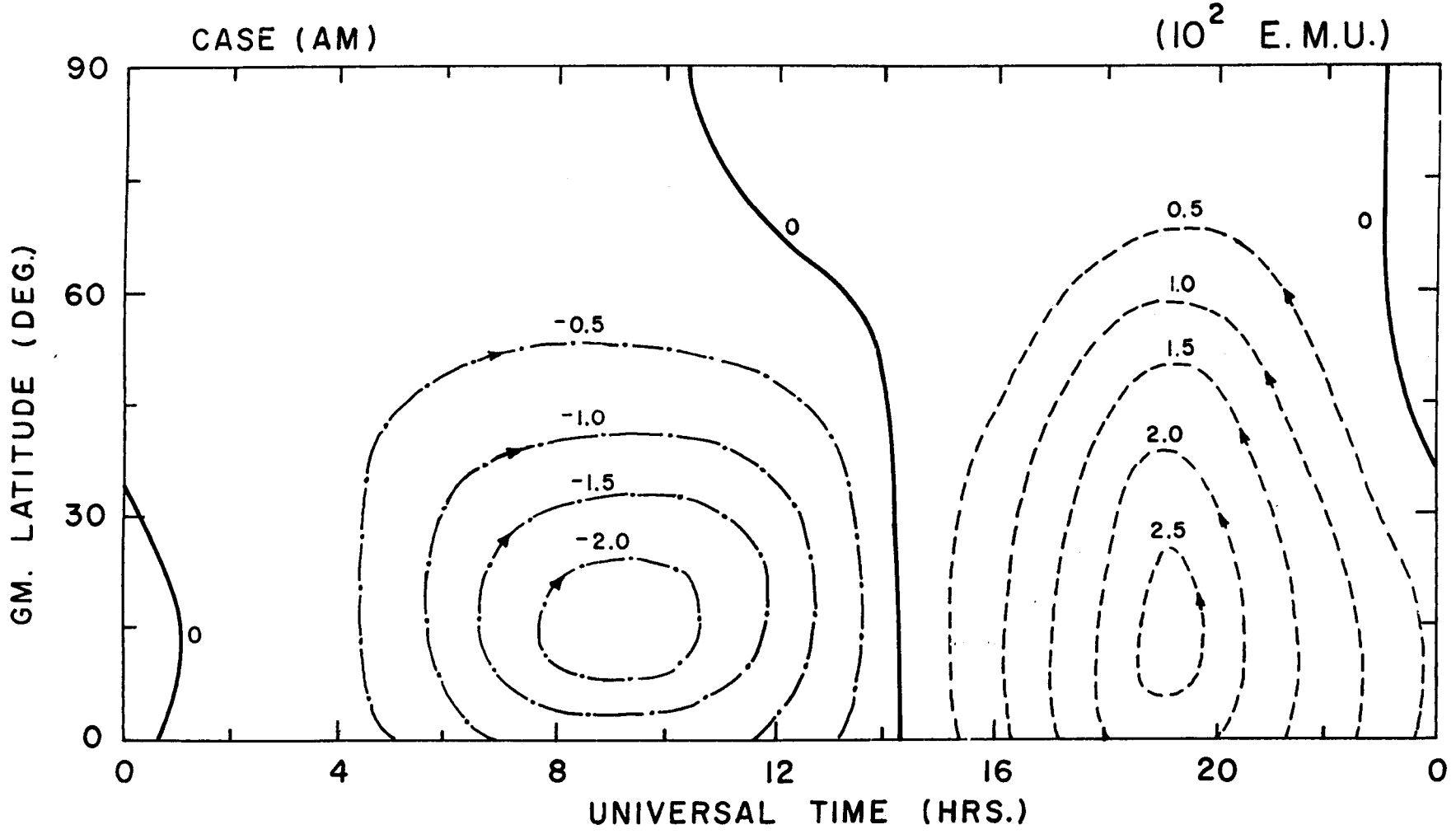
CASE (AM)
(10² E.M.U.)
90
60
30
0
GM. LATITUDE (DEG.)
0
-0.5
-1.0
-1.5
-2.0
0
0.5
1.0
1.5
2.0
2.5
0
0
4
8
12
16
20
0
UNIVERSAL TIME (HRS.)

Fig. 8C.